The Journal of Experimental Biology 206, 3337-3348

doi:10.1242/jeb.00571

The retina of *Manduca sexta*: rhodopsin expression, the mosaic of green-, blue- and UV-sensitive photoreceptors, and regional specialization

Richard H. White[1,*], Huihong Xu[2], Thomas A. Münch[3], Ruth R. Bennett[1] and Erin A. Grable[1]

[1]*Department of Biology, University of Massachusetts Boston, 100 Morrissey Blvd, Boston, MA 02125-3393, USA,* [2]*MGH Cancer Center, Harvard Medical School, 13th Street, Charlestown, MA 02129, USA* and [3]*Helen Wills Neuroscience Institute, University of California Berkeley, 145 Life Sciences Addition, Berkeley, CA 94720, USA*

*Author for correspondence (e-mail: richard.white@umb.edu)

Accepted 25 June 2003

Summary

Spectral sensitivities of individual photoreceptors in the compound eye of *Manduca sexta* were verified by immunocytochemistry, and the retinal mosaic was mapped, using polyclonal antisera raised against amino-terminal sequences of three identified rhodopsins: P520, P450 and P357. Retinulae are composed of a small proximal cell and seven or eight elongate cells extending across the retina. In each retinula, one or two elongate *dv* cells oriented in the dorsal–ventral axis of the retinal lattice express either P450 or P357. Six elongate *ap* and *ob* cells in the anterior–posterior and oblique axes express P520. The small proximal *pr* cell also appears to express P520. The retinal mosaic is regionalized into three distinct domains: ventral and dorsal domains that divide the main retina, and a large dorsal rim area. The immunocytochemical data provide a high-resolution map of the *Manduca* retina that confirms and refines earlier low-resolution ERG spectral sensitivity measurements. The dorsal and ventral domains, separated at a well-defined equatorial border, are distinguished by differences in the proportion of blue-sensitive *dv* cells: these cells dominate the ventral retina but are less abundant in the dorsal retina. Green-sensitive *ap* and *ob* receptors are uniformly distributed across the dorsal and ventral domains, and UV-sensitive *dv* cells are fairly uniformly distributed because many retinulae in the dorsal domain contain only one *dv* cell. Similarly, dorsal rim retinulae contain only the ventral member of the *dv* pair of receptors, two-thirds of which express P357. Otherwise, dorsal rim receptors express none of the three sequenced *Manduca* opsins; they must express rhodopsins that have yet to be cloned.

Key words: Sphingidae, *Manduca sexta*, rhodopsin, retinal mosaic, regionalization, dorsal rim.

Introduction

Most sphingid moths, as exemplified by *Manduca sexta*, are crepuscular or nocturnal foragers. They feed on the nectar from flowers that are typically white or palely colored but do not reflect wavelengths below 400 nm (White et al., 1994; Cutler et al., 1995). The spectral sensitivity curve of spontaneous foraging shows a prominent peak in the blue at 450 nm with a minor peak in the green at 530 nm; wavelengths below 400 nm in the ultraviolet inhibit or interfere with foraging (Cutler et al., 1995). Electroretinogram (ERG) spectral sensitivity measurements indicate that green-sensitive (G) and UV-sensitive (UV) photoreceptors are distributed uniformly across the retina, whereas blue-sensitive (B) receptors are located only or mainly in the ventral retina. From these results, we hypothesized that the ventral retina is functionally specialized for flower localization and foraging behavior (Bennett et al., 1997).

The spectral sensitivity of foraging is consistent with our knowledge of the visual pigments expressed in the retinal photoreceptors of *Manduca*. Three rhodopsins – P520, P450 and P357 – have been characterized by spectrophotometry, ERG spectral sensitivity and the cloning of three opsin cDNAs (White et al., 1983; Bennett and Brown, 1985; Chase et al., 1997; Bennett et al., 1997). The G and UV photoreceptors expressing P520 and P357 were identified by electron microscopy (EM) through the structural effects of intense colored light, but the B cells expressing P450 were not found (Cutler et al., 1995). Here, we confirm the identity of the G and UV receptors and identify the B receptors by opsin immunocytochemistry. This approach has also provided a map of the retinal mosaic of photoreceptors that refines our low-resolution ERG data. Our aim is to examine more precisely the hypothesis that B receptors, predominant in spontaneous foraging behavior, are localized to the ventral retina.

Materials and methods

Animals

Manduca sexta L. were reared on a carotenoid-rich artificial diet under conditions described previously (Bennett and White, 1989).

Antisera

Three *Manduca* opsin cDNA sequences were cloned from retinas and identified by Chase et al. (1997): MANOP1 encodes P520; MANOP2, P357; MANOP3, P450. Rabbit anti-opsin antibodies were generated to the three *Manduca* opsins. The amino terminus of MANOP2 with added His.Tag sequence, 5′-TNFTQELYEIGPMAYPLKMISKDVAEHML-GWNIPEEHQDLVHDHWRNFPAVSKYWHTALALLYIFF-TFAALVGHHHHHH-3′, was expressed in BL21 (DE3) NovaBlue *Escherichia coli* with the expression plasmid vector pET-30a (Novagen, Madison, WI, USA). One hour after induction, a peptide of appropriate molecular mass (9.8 kDa) appeared on SDS–PAGE gels of total protein from culture samples. The expressed target peptide was purified through a Novagen His.Bind column under denaturing conditions, run on a 22% SDS–PAGE gel, and the target band was excised. Rabbit antisera to the excised gel band were prepared by Charles River PharmServices (Wilmington, MA, USA). As similar efforts to express P520 and P450 failed, short synthesized peptides from amino-terminal segments were used to raise antisera against these opsins: P520, 3′-DPHWYQF-PPMNPLWH-5′; P450, 3′-EEHQDLVHDHWRNFPAVSK-5′. Peptides and antisera were provided by Zymed Laboratories (San Francisco, CA, USA).

Antisera were assessed from western blots of retinal extracts subjected to SDS–PAGE electrophoresis. Dissected retinas were ground in 0.1 mol l^{-1} phosphate buffer, pH 7, with 1 mmol l^{-1} EDTA (Sigma, St Louis, MO, USA) and centrifuged at 16 000 ***g***. The pellet was washed in phosphate buffer to remove solubilized screening pigment and extracted in SDS (Sigma). Following centrifugation, aliquot parts of supernatant were subjected to SDS–PAGE electrophoresis with pre-stained molecular mass standards (Bio-Rad, Hercules, CA, USA). Western blots (blocked with 5% bovine serum albumin) were prepared with the ABC reagents from Vector Laboratories (Burlingame, CA, USA). Blots were stained with 4-chloro-1-napthol in ethanol mixed with peroxide buffer (Sigma).

Immunocytochemistry

Retinas were fixed in phosphate-buffered 4% paraformaldehyde and cut into various pieces along the anterior–posterior and dorsal–ventral axes. Retinal pieces were oriented in paraffin blocks and sectioned at 6 µm. An ABC peroxidase immunostaining protocol with VIP substrate (provided in kits from Vector Laboratories) was used for localizing opsins to individual retinulae and receptor cells (intense autofluorescence precluded fluorescent tags). Digital images of sections were collected by Scion Image software from an Olympus BX60 microscope. Localization of the three opsins was compared in adjacent sections. During histological processing, retinas fractured randomly along the tracheole palisades that separate the retinulae; the resulting uniquely shaped blocks of retinulae greatly facilitated precise alignment of adjacent sections.

Retinal morphology

Isolated retinas were fixed in cacodylate-buffered glutaraldehyde–formaldehyde and processed according to standard procedures (White and Bennett, 1989). Thick sections were photographed in a Zeiss WL compound microscope, and thin sections in a Philips 300 electron microscope. Whole retinas and hand-cut sections were photographed in a Wild M5 stereomicroscope.

Rhabdomere volumes

Morphology and volumes of the rhabdomeres of the different classes of *Manduca* photoreceptors were determined as follows. A single tangential electron microscope section was chosen that extended from the distal surface of a retina to below the proximal basement membrane near the center of the retina. Low-magnification electron micrographs were taken of a complete set of tangentially sectioned retinulae in two parallel rows, to provide a composite of 21 profiles of retinulae distributed across the full width of the retina (Fig. 1A). In order to determine the plane of this tangential section across the retina, a line was projected on a light micrograph of a longitudinal section from a different retina that intersected 11 retinulae, the number in the longest row of electron micrographs (Fig. 1B). From this, the actual depth of each profile could be determined. The profiles were then treated as thick, virtual, serial cross-sections of a single retinula from

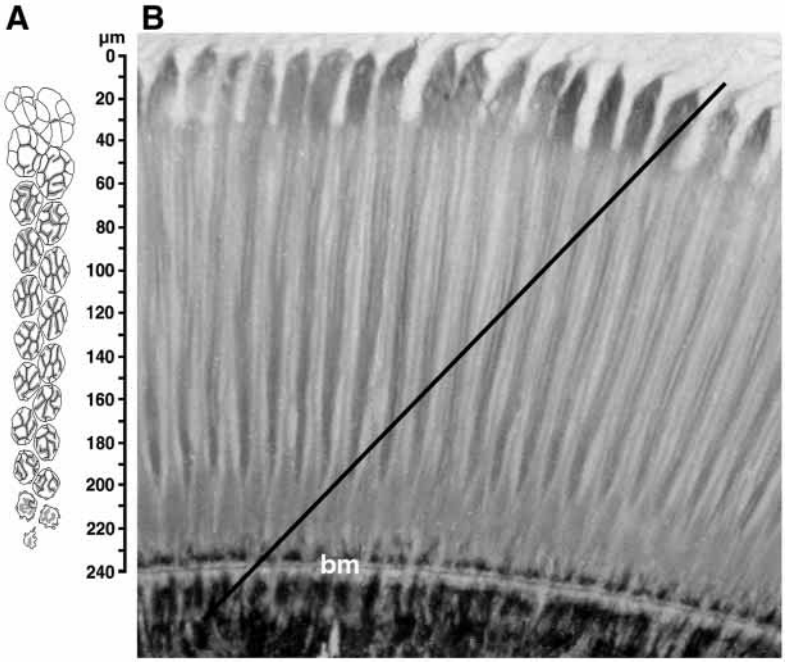

Fig. 1. Illustration for method of measuring rhabdomere volumes. (A) Profiles (see Fig. 5A) of two adjacent rows of retinulae traced from electron micrographs of a tangential section extending from the retinal surface to the basement membrane. (B) Inferred plane of section projected across a light micrograph of a longitudinally sectioned retina.

which rhabdomere volumes could be estimated. Corresponding cells were identified from their positions in the photoreceptor rosette in each sectioned retinula, and the areas of their rhabdomeres were measured and appropriately adjusted downward to compensate for profile elongation resulting from the tangential cut. To summarize, this procedure enabled the reconstruction, from a single tangential section, of a set of virtual serial sections, for which thickness dimensions could be inferred and within which rhabdomere areas could be measured. Rhabdomere volumes for each cell type were calculated from these values.

Results

Organization of the Manduca *compound eye*

Manduca has a typical lepidopteran superposition eye. We calculated that the eye is composed of approximately 27 000 facets based on counts from isolated corneas. Facet diameter (30.3±1.8 μm, mean ± S.E.M.) varied little across the cornea. Screening pigment is restricted to the primary pigment cells enclosing the crystalline cones, the distal ends of the secondary pigment in the clear zone and the small proximal ends of the secondary pigment cells at the basement membrane (Banister and White, 1987). Receptor cells contain no ommochrome granules.

When the retina is exposed by cutting away the cornea and associated pigment, it appears irregularly yellow to orange, except for a large, distinctive dorsal rim area, which has a more transparent bluish appearance (Fig. 2A). We will refer to the main retina as the 'yellow retina' to distinguish it from the dorsal rim. Since the retinas of carotenoid-deprived moths are white, the yellow color presumably results from carotenoids deposited in the retina (Bennett and White, 1989).

From its area, approximately 0.25 mm^2, we estimate that the dorsal rim contains about 1000 retinulae. Two factors may account for its distinctive appearance. Perhaps it contains less carotenoid. In addition, there is a difference in the tapetum that is responsible for the eye glow of the dark-adapted eye (Banister and White, 1987). The tapetum is provided by tracheoles that branch into the retina from a single tracheal cell that underlies each retinular unit. In the yellow retina, the tracheole branches extend nearly to the surface of the retina (Figs 2B,C, 3A, 4B), densely surrounding and isolating each retinula from its neighbors. In the dorsal rim area, the tracheoles terminate just above the basement membrane (Figs 2B,D, 4A). The blue cast of the retina may come from underlying screening pigment made visible by the reduced tracheal tapetum.

Each retinula is made up of a small proximal cell and seven or eight elongate photoreceptor cells that span the full depth of the retina. Morphological details of retinulae in the yellow retina and the dorsal rim area are presented in Fig. 5. The elongate cells can be distinguished by characteristic morphologies and their positions relative to the axes of the hexagonal lattice of the compound eye (Cutler et al., 1995). There are one or two *dv* cells (either the dorsal or ventral member of the pair may be missing: Carlson et al., 1967; Cutler et al., 1995) oriented in the dorsal–ventral axis of the retina; two *ap* cells in the anterior–posterior axis; and four oblique *ob* cells. In the yellow retina, the rhabdomeres of *dv* cells are restricted to the distal half of the retinula. The rhabdomeres of the *ap* and *ob* cells extend most of the length of the retinula but have distinctive rhabdomere morphologies (Fig. 3). The proximal *pr* cell lies at the center of the retinula just above the

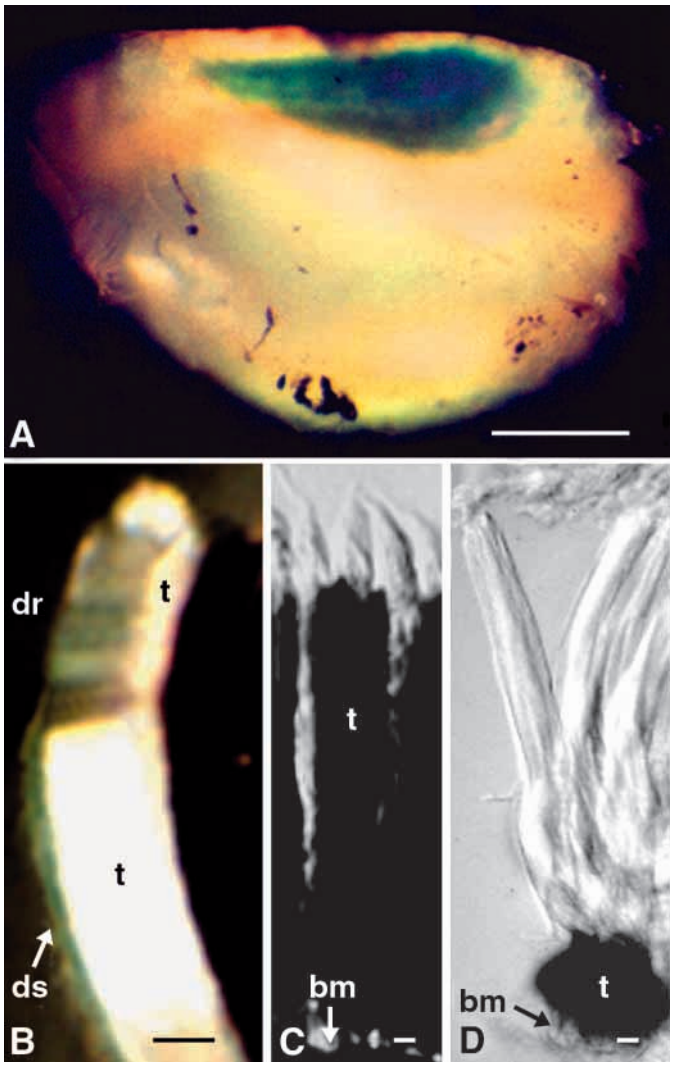

Fig. 2. Retina of *Manduca sexta*. (A) Dorsal aspect of an unfixed retina dissected free of the cornea and clear zone. Anterior is to the right. The blue patch is the dorsal rim area. Scale bar, 0.5 mm. (B) Freehand vertical section of a glutaraldehyde-fixed retina photographed in reflected light. Dorsal is at the top, distal to the left. The highly reflective tracheoles (t) extend almost to the distal surface (ds) of the retina, except in the dorsal rim area (dr). Scale bar, 100 μm. (C) Retinulae dissected from the center of a fixed retina photographed in transmitted light: tracheoles are opaque, extending across the retina to just below the distal tips of the retinulae. bm, basement membrane beneath the retina. Scale bar, 10 μm. (D) Dorsal rim retinulae. Tracheoles envelop only the proximal ends of the retinulae. Scale bar, 10 μm.

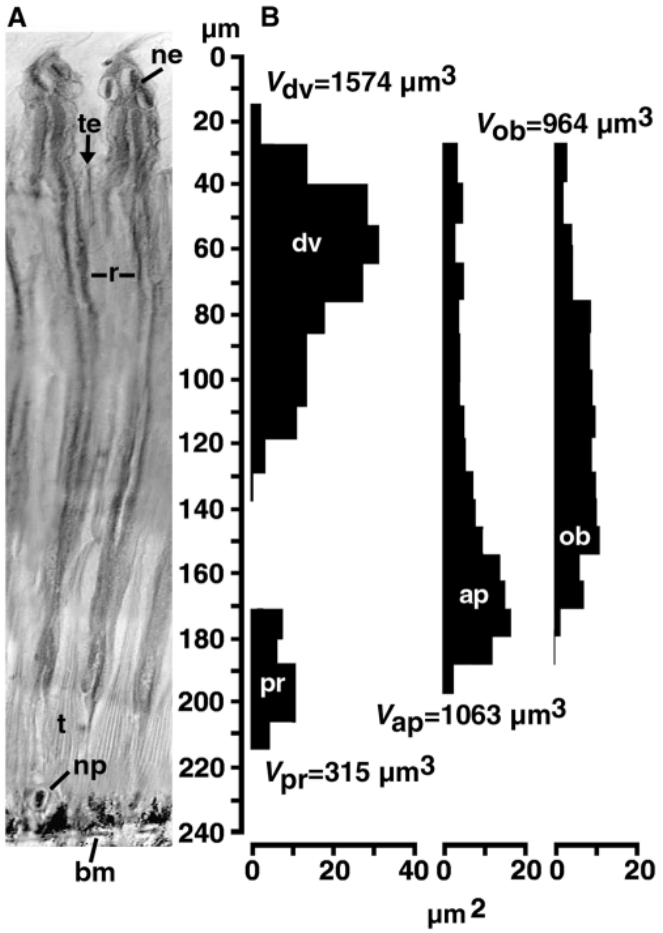

Fig. 3. Rhabdomere volumes of receptor cells near the center of the retina. (A) Light micrograph of longitudinal section showing two retinulae. bm, basement membrane; ne, nuclei of elongate photoreceptors; np, nucleus of small proximal receptor; r, rhabdom; t, tracheoles; te, tracheole ends. (B) Rhabdomere volumes, calculated from 21 virtual sections (see Materials and methods and Fig. 1A) of photoreceptors in relation to depth of retina. Each rectangle represents a virtual section: its vertical side represents the section thickness; the horizontal side represents the area of the rhabdomere. The calculated rhabdomere volume for each cell type is indicated.

basement membrane with its rhabdomere on either side in the anterior–posterior axis. Electron micrographs of *Manduca* retinulae can be found in Cutler et al. (1995) and earlier papers cited therein. Rhabdomere volumes (Fig. 3) were estimated for each morphological class of receptor, as outlined in Materials and methods, from the set of 21 retinulae shown in Fig. 1: *dv* cell, 1574 μm^3; *ap* cell, 1063 μm^3; *ob* cell, 964 μm^3; *pr* cell, 315 μm^3.

The same set of elongate receptors can be recognized in dorsal rim retinulae from their orientations; however, only the ventral *dv* cell is present. Rhabdomere organization is also distinctive: microvilli are oriented orthogonally; those of the *ob* and narrow *dv* cells parallel to the dorsal–ventral axis of the eye, those of the *ap* cells parallel to the anterior–posterior axis (Fig. 5B). From a limited EM study, we found that this structure is preserved down the full length of the retinula. We have not determined whether or not a *pr* cell is present.

Assessment of anti-opsin antisera

Fig. 6 shows western blots of the three rhodopsin antisera. There is a major band in each rhodopsin lane at approximately 37 kDa, as expected (Bennett and White, 1989; Chase et al., 1997). Antisera immunostained specific rhabdomeres in retinal sections with little background. Rhabdomeres were not stained above background in control sections processed without primary or secondary antibodies.

Localization of opsins to receptor cells

In longitudinal sections of the yellow retina, anti-P520 was seen to stain rhabdoms from just below the distal surface of the retina to just above the basement membrane (Fig. 7A), where the rhabdomeres of the *ap*, *ob* and *pr* cells are found. Anti-P450 and anti-P357 stained the rhabdom distally, where the rhabdomeres of the *dv* cells are located (Fig. 7B,C).

Cross-sections provided precise identification of immunolabeled cell types. Fig. 8 compares staining for P520 and P357 in adjacent sections from about 70 μm below the retinal surface. Anti-P357-stained rhabdomeres oriented in the dorsal–ventral axis of the retina (Fig. 8B), whereas anti-P520-stained rhabdomeres oriented on either side (Fig. 8A). Comparison of this pattern with the EM image of a retinula at a similar depth in the retina (Fig. 5A; 70 μm) confirms that P357 is expressed by *dv* cells and P520 by *ap* and *ob* cells. However, Fig. 8B also

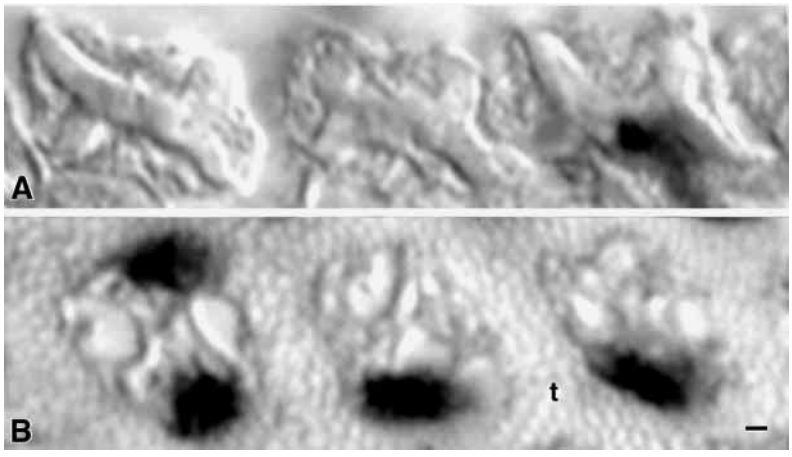

Fig. 4. Comparison of dorsal rim retinulae with nearby retinulae of the yellow retina in the same section stained with anti-P357 and photographed with phase interference optics to enhance images of rhabdoms. (A) Dorsal rim retinulae with typical butterfly-shaped rhabdoms. Note the absence of surrounding tracheoles. The narrow ventral *dv* cell is stained in the retinula on the far right. (B) Retinulae surrounded by tracheoles (t) from an adjacent region of the yellow retina. Two *dv* cells are stained in the retinula on the far left; only one cell is stained in the other retinulae. Scale bar, 1 μm.

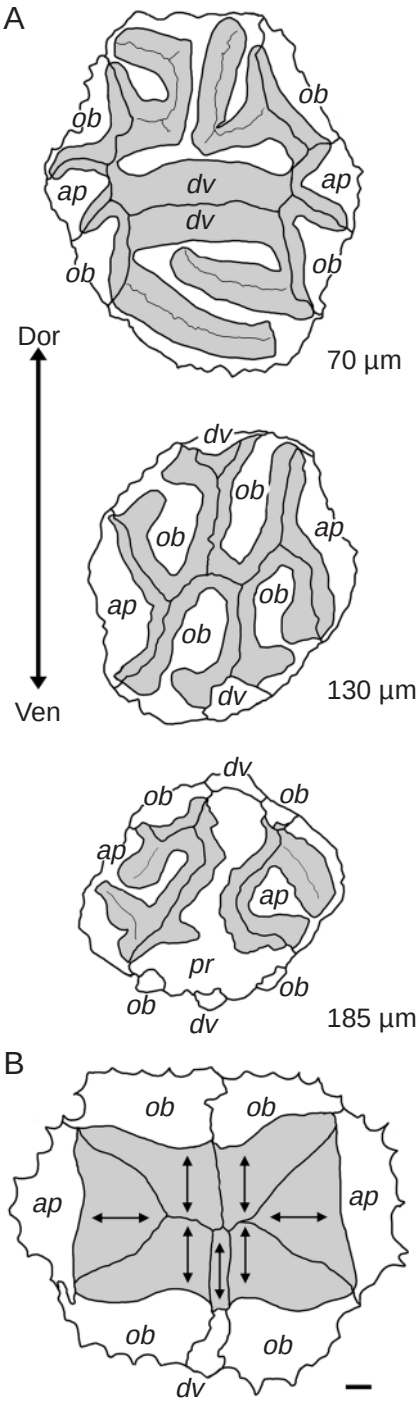

Fig. 5. Organization of retinulae from the yellow retina and dorsal rim. (A) Tracings of electron micrographs from sectioned retinulae near the center of the retina, showing the component photoreceptors and their rhabdomeres (shaded). The dorsal–ventral axis of the retina is vertical. The depth of each retinular profile from the surface of the retina (see Fig. 3) is indicated. *dv*, dorsal–ventral receptor cells; *ap*, anterior–posterior cells; *ob*, oblique cells; *pr*, proximal cell. (B) Tracing from electron micrograph of a retinula from the dorsal rim area. The structures of the eight elongate receptor cells do not vary with retinal depth (the basal *pr* cell has not yet been found). Only the ventral *dv* cell is present. Orientations of photoreceptor microvilli are indicated by double-headed arrows. Scale bar, 1 µm.

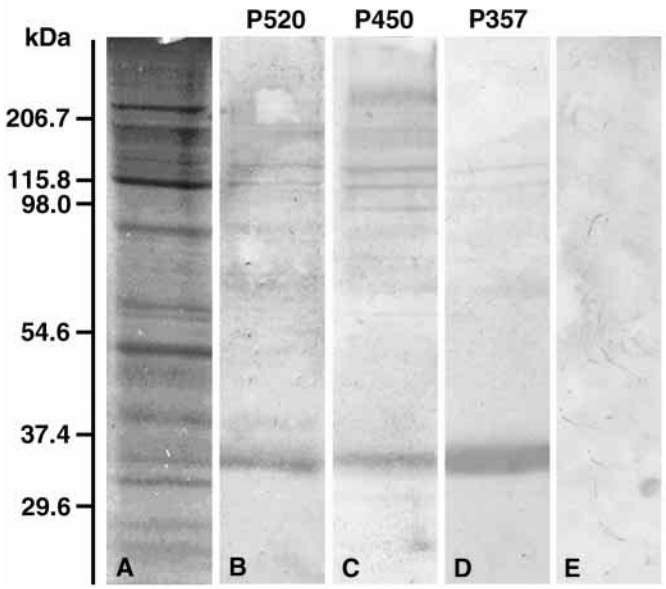

Fig. 6. Proteins from *Manduca* retina. (A) SDS–PAGE electrophoresis of aliquot parts of retinal homogenate equivalent to 0.1 retina, calibrated with molecular masses of Bio-Rad protein standards. (B,C,D) Western blots with antisera against P520, P450 and P357, respectively, showing a major band at approximately 37 kDa. (E) Control blot lacking primary antibodies.

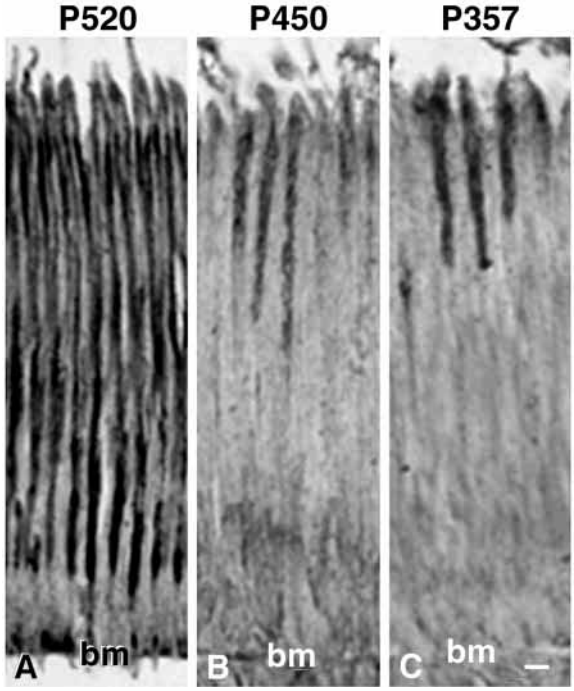

Fig. 7. Longitudinal sections from the same retina immunostained with antisera to the three characterized *Manduca* opsins. (A) Anti-P520. (B) Anti-P450. (C) Anti-P357. The dark blotches just above the basement membrane (bm) in A are screening pigment, not stain. Scale bar, 10 µm.

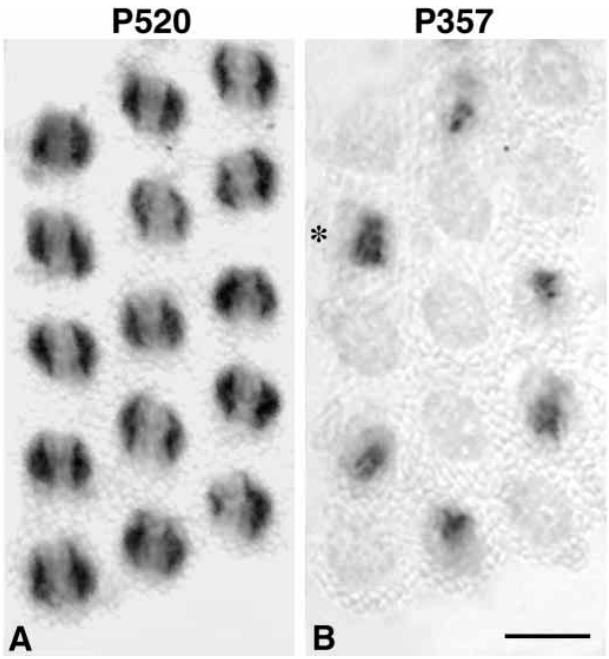

Fig. 8. Adjacent immunostained sections from the ventral domain of the retina, approximately 70 μm from the surface of the retina. The dorsal–ventral retinal axis is vertical. (A) Anti-P520. Rhabdomeres of *ap* and *ob* cells are stained. (B) Anti-P357. Some *dv* cells are stained. A retinula in which both *dv* cells are stained is marked with an asterisk. Scale bar, 10 μm.

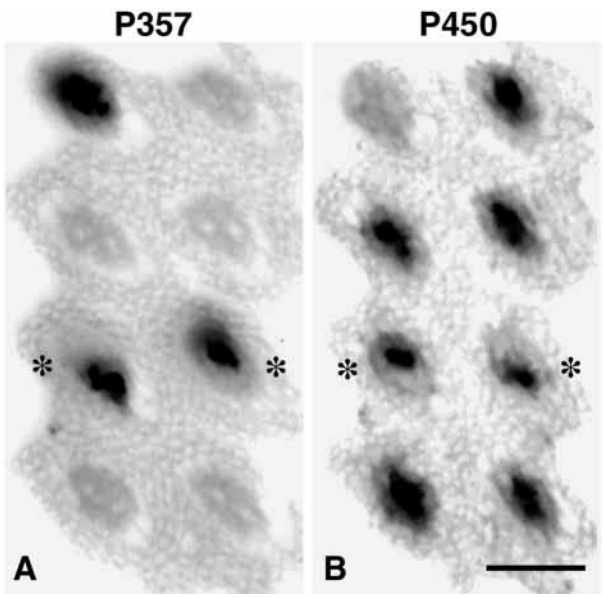

Fig. 9. Adjacent immunostained sections from the ventral domain of the retina. (A) Anti-P357. (B) Anti P-450. Asterisks mark retinulae in which one *dv* cell stains for P357, the other for P450. Scale bar, 10 μm.

indicates that that many *dv* cells express neither P357 nor P520. Adjacent sections stained with anti-P357 or anti-P450 (Fig. 9) show that *dv* cells express either P357 or P450. No instances were found in which more than one rhodopsin was expressed in the same cell, as reported in the butterfly *Papilio xuthus* (Kitamoto et al., 1998). To summarize, *ap* and *ob* cells are green-sensitive (G) receptors expressing P520; *dv* cells are either blue-sensitive (B) or UV-sensitive (UV) receptors expressing P450 or P357, respectively.

Close examination of longitudinally sectioned retinulae strongly suggested that the proximal *pr* cell also expresses P520, but its small rhabdomere cannot be distinguished with certainty in the light microscope. It certainly does not express either P357 or P450.

Neither P520 nor P450 was expressed in dorsal rim retinulae. However, some of the ventral *dv* cells stained for P357 (Fig. 4A).

Regionalization

The pattern of expression of the three opsins was examined in samples from all sectors of the retina. P520 was expressed uniformly in *ap* and *ob* cells in all regions of the yellow retina but was not expressed in the dorsal rim area. Regional differences in the expression of P357 and P450 in *dv* cells of the yellow retina are shown in Tables 1, 2 and Fig. 10. The immunocytochemical data summarized in Table 1 were gathered from retinas cut into quadrants along the dorsal–ventral and anterior–posterior axes. As no anterior–posterior differences were found, the data for dorsal quadrants are combined, as are those from ventral quadrants. The dorsal and ventral densities of *dv* cells expressing P357 were similar: approximately 60 cells per 100 retinulae. However, cells expressing P450 were much more abundant in ventral retinas: approximately 140 receptors per 100 ventral retinulae compared with approximately 35 receptors per 100 dorsal retinulae.

Detailed maps of the retinal mosaic were assembled from three sets of exceptionally well-stained adjacent sections from three different retinas showing large patches of retinulae from dorsal, central and ventral regions (Fig. 10; Table 2). Fig. 10C shows a portion of a larger ventral patch; almost all retinulae in this region had two *dv* cells, with B cells that expressed P450 predominantly. 69% of the *dv* cells were B receptors, giving a density of 137 B cells and 62 UV cells per 100 retinulae.

Fig. 10B shows the dorsal patch, which included retinulae

Table 1. *Densities of* dv *photoreceptor cells*[1] *expressing either P450 or P357 in dorsal and ventral halves of the central retina of* Manduca sexta

	Dorsal[2]	Ventral
dv cells expressing P450	35±9.3 (6)	139±18.6 (8)
dv cells expressing P357	63±9.4 (7)	57±15.9 (8)

Values are means ± S.E.M. (sample size is given in parentheses).
[1]Number of stained cells per 100 retinulae.
[2]Dorsal rim not included.

Table 2. *Distribution of* dv *photoreceptor cells expressing either P450 or P357 (from Fig. 10) in central domains of the retinal mosaic of* Manduca sexta

		Equatorial patch		
	Dorsal patch[1]	Dorsal	Ventral	Ventral patch
Number of retinulae	554	341	216	1112
Retinulae with two stained *dv* cells	12	177	171	1107
Retinulae with one stained *dv* cell	516	155	41	5
Retinulae with no stained *dv* cells	26	9	4	0
Number of stained *dv* cells	540	509	383	2219
dv cells expressing P450	184	130	254	1524
dv cells expressing P357	356	379	129	695
Density of blue-sensitive cells[2]	33.2	38.1	117.6	136.9
Density of UV-sensitive cells[2]	64.3	111.1	59.7	62.4

[1]Dorsal rim area not included.
[2]Number of stained cells per 100 retinulae.

from both the yellow retina and dorsal rim. Here, only one *dv* cell was stained in most retinulae at the dorsal edge of the yellow retina, with 66% of stained cells expressing P357. In addition, a number of retinulae showed no stained *dv* cells. The densities of B and UV receptors were 33 and 64 cells per 100 retinulae, respectively.

The patch from the middle of the retina (Fig. 10D,E) showed that a distinct equatorial border separates the predominantly UV-sensitive dorsal and predominantly blue-sensitive ventral halves. Below this border, most retinulae have two *dv* cells, 66% of which express P450. The densities of B and UV receptors were 118 and 60 cells per 100 retinulae, respectively. On the dorsal side of the border, half of the retinulae had only one *dv* cell, and 74% expressed P357. The densities of B and UV receptors were 38 and 111 cells per 100 retinulae, respectively.

In the portion of the dorsal rim area shown in Fig. 10B, about one-third of 124 retinulae showed *dv* cells that expressed P357, while none expressed P450. 65% of 2125 retinulae from five larger dorsal rim samples (data not shown) contained a cell expressing P357. As all dorsal rim retinulae surveyed in electron micrographs contained a ventral *dv* cell, the lack of P357 expression does not reflect the absence of *dv* cells from unstained retinulae. None of the dorsal rim *ap* and *ob* cells was stained by antisera to any of the three opsins.

Discussion

Organization of retinulae

The organization of the *Manduca* retinula is similar to that of *Deilephila elpenor* (Welsch, 1977; Schlecht, 1979; Schlecht et al., 1978) and other sphingids (Eguchi, 1982). It is a variant of the basic architecture of the lepidopteran retinula (Johnas, 1910; Gordon, 1977; Kolb, 1977, 1985, 1986; Maida, 1977; Ribi, 1978, 1987; Shimohigashi and Tominaga, 1986, 1991, 1999; Bandai et al., 1992; Kitamoto et al., 2000; Kelber et al., 2001; Qiu et al., 2002; Briscoe et al., 2003), whose constituent cells have been designated by numbering schemes, notably that of Ribi (1978), in which *dv* cells are 1 and 2, *ap* are 3 and 4, *ob* are 5, 6, 7 and 8, and the *pr* cell is 9.

The distinctive features of *Manduca* dorsal rim retinulae indicate that they function, as in other insects, for perception of polarized light (Kolb, 1986; Labhart and Meyer, 1999; Labhart et al., 1992, 2001): rhabdoms have orthogonally oriented microvilli for analyzing the plane of polarization, and retinulae lack mutually isolating features such as screening pigment or tracheole sheaths to enable large visual fields. The dorsal rim area of *Manduca* is remarkable for its large size, encompassing about 1000 retinulae. It seems likely that this is an adaptation for the unique behavioral ecology of such crepuscular/nocturnal sphingids; they are strong flyers that navigate over long distances under dim light (Janzen, 1984; Haber and Frankie, 1989). Similar dorsal rim areas have been reported for other moth species [the sphingid *Deilephila elpenor*, the noctuids *Spodoptera exempta* and *Plusia gamma* (Meinecke, 1981) and the saturnid *Anthera polyphemus* (Anton-Erxleben and Langer, 1988)].

Spectral classes of photoreceptors

The classification of *Manduca* photoreceptors depends on the proper assignment of the cDNA sequences used to generate anti-opsin antisera. As the opsin-encoding cDNAs isolated from *Manduca* retinas have not been expressed, their initial identification was based mainly on similarities to other arthropod opsin sequences (Chase et al., 1997). Our conclusion that MANOP1 encodes P520, MANOP3, P450 and MANOP2, P357 has been strengthened by the subsequent isolation of more insect opsin sequences (Briscoe, 1998, 2000, 2001; Briscoe and Chittka, 2001) and confirmed by the results presented here. We have verified, in particular, the assignment of the similar MANOP2 and MANOP3 sequences to the P357 and P450 rhodopsins, respectively. Antisera to an expressed fragment of MANOP2 mark the distal rhabdomeres of *dv* cells that were previously identified as UV receptors in *Manduca* (Cutler et al., 1995) and in the similar retina of the sphingid

Deilephila (Schlecht et al., 1978; Schlecht, 1979) through the morphological effects of light. Furthermore, we show that MANOP3-expressing *dv* cells are concentrated in the ventral retina where B cells are localized (Bennett et al., 1997), whereas MANOP2 expression, like UV sensitivity, is more uniformly distributed.

Our conclusions for *Manduca* are corroborated by similar analyses of opsin expression in the compound eyes of the

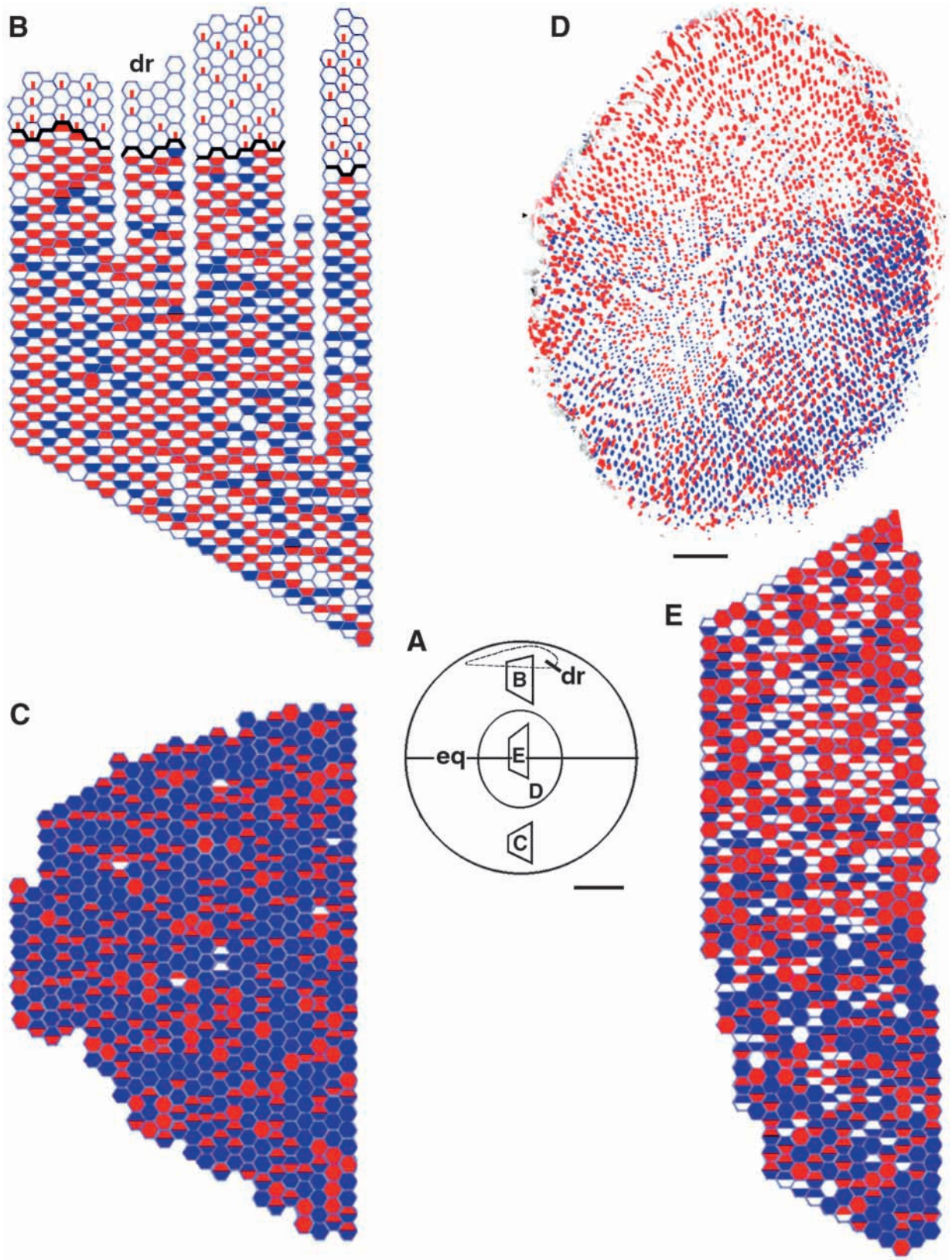

butterflies *Papilio xuthus* (Kitamoto et al., 1998, 2000) and *Vanessa cardui* (Briscoe et al., 2003). Receptors corresponding to *Manduca dv* cells express homologous blue- and UV-sensitive rhodopsins; those corresponding to *ap* and *ob* receptors express P520 homologs. Although the small *pr* cell in the *Manduca* retina cannot be clearly distinguished by light microscopy, it also appears to express P520. This conclusion is strengthened by the expression of P520 homologs in the corresponding cells of *Papilio* and *Vanessa*.

Retinal mosaic

The division of the *Manduca* retina into distinct dorsal and ventral domains seems a common, perhaps basic, feature in the differentiation, morphology and function of the insect compound eye (White, 1961; Stavenga, 1992; Wolff and Ready, 1993; Kitamoto et al., 1998; Briscoe et al., 2003).

Nearly all retinulae near the ventral margin of the eye have two *dv* cells (Table 2; Fig. 10C). Retinulae showing only one stained cell are frequent in the dorsal half of the retina. We cannot tell with light microscopy if they actually have only a single *dv* cell, but electron microscopy (micrographs not shown) qualitatively supports this inference. However, it is possible that some of these retinulae may include two *dv* cells, one of which expresses an as yet unidentified rhodopsin. This suspicion arises because some retinulae, especially dorsally (Table 2; Fig. 10B), stain for neither P450 nor P357, and, as deduced below for the dorsal rim area, we clearly have not identified all the rhodopsins of the *Manduca* retina. Although retinulae lacking both *dv* cells have not been detected in electron micrographs, they easily would have been missed. Retinulae with one stained *dv* cell become more frequent towards the dorsal edge of the ventral domain and increase across the dorsal domain. In the equatorial region, stained dorsal and ventral *dv* receptors are randomly distributed among one-celled retinulae. Towards the dorsal edge of the dorsal domain, more than 90% are ventral cells, the same asymmetry seen in adjacent dorsal rim retinulae (Fig. 10B).

The density of B and UV receptors (against a uniform background of G receptors), expressed as number of cells per 100 retinulae, is shown in Table 1: in the dorsal retina, 35 B and 63 UV; ventrally, 139 B and 57 UV. B cells dominate the ventral domain and are reduced, but not missing, as suggested by Bennett et al. (1997), from the dorsal domain. UV cells, like G cells, are fairly evenly distributed across the retina except for a region of higher density just above the equator. There is no obvious pattern in the local distribution of B and UV receptors in either domain. The question of pattern can be examined quantitatively in the ventral patch shown partially in Fig. 10C, where nearly all retinulae have two *dv* cells. B and UV cells are randomly distributed among dorsal and ventral pairs, with 537 B/B, 449 B/UV and 121 UV/UV, i.e. a binomial distribution ($P>0.2$) in which the frequency of B and UV cells is 0.69 and 0.31, respectively. The details of the mosaic of *dv* receptors (Table 2; Fig. 10) suggest two mechanisms that might control elaboration during retinal differentiation. First, differing relative strengths in each domain of determinants that, acting randomly on nascent *dv* cells, specify the alternative expression of P450 or P357. Secondly, the deletion or developmental arrest of some *dv* cells, an action that is prominent in the dorsal domain and is graded from dorsal to ventral. The combined operation of these mechanisms could result in the observed features of the mosaic. First, a high density of B receptors in the ventral domain and a low density of B receptors in the dorsal domain resulting from the different balances between determinants in each domain. Second, a fairly uniform density of UV receptors across both domains, but with a region of higher density towards the equatorial margin of the dorsal domain, resulting from the gradient of *dv* cell deletion. It will be informative to map the retina during its pupal differentiation.

In previous studies, we estimated the relative proportions of the three visual pigments in the *Manduca* retina from measurements of rhodopsin absorption and ERG spectral sensitivities. The most recent, and we believe most accurate, estimates were based on fitting rhodopsin nomograms to ERG spectral sensitivity measurements from dorsal and ventral regions of the retina (Bennett et al., 1997). From the data presented here, we can now estimate these values in a completely different way, under the different assumptions described in the Appendix, by combining receptor cell densities and rhabdomere volumes.

In the dorsal domain, the ratio of the three rhodopsins (P520:P450:P357) ranges from 80:7:13 to 73:7:20; in the ventral domain, it ranges from 67:23:10 to 69:20:10. These values may be compared with those derived from the ERG spectral sensitivity curves: dorsally, 88:0:12; ventrally, 62:19:19 (Bennett et al., 1997). The similarity of rhodopsin ratios yielded by these different methods strengthens our conclusions.

Fig. 10. Retinal mosaic of blue- and UV-sensitive photoreceptors. (A) Diagram of the *Manduca* retina drawn to scale, showing locations of the retinal patches illustrated in B–E. Anterior is to the right. The equatorial division (eq) between dorsal and ventral retinal domains is indicated, as is the dorsal rim area (dr). Scale bar, 0.5 mm. (B,C,E) Diagrammatic representations of retinal patches mapped from adjacent sections stained for P450 and P357, respectively. Each hexagon represents a retinula containing potentially two *dv* cells. A uniformly colored hexagon represents a retinula containing two identical cells. A hexagon divided in half horizontally is a retinula with unlike or missing cells. Blue represents cells expressing P450; red represents cells expressing P357; white indicates no staining by either antiserum in that position. (B) Domain in the dorsal retina that extends into dorsal rim region (dr), whose margin is represented by the heavy line. Some dorsal–ventral rows of retinulae terminate before reaching the edge of the retina. Red lines in the dorsal rim region represent the narrow *dv* cells that express P357. (C) Domain in the ventral retina. (D) Large patch at the center of the retina for which grayscale micrographs of adjacent sections immunostained for P450 and P357 have been superimposed and arbitrarily colored (blue, anti-P450; red, anti-P357) in Adobe Photoshop. Scale bar, 100 μm. (E) Equatorial sector from the adjacent sections shown in D.

The photoreceptors in the retina of the butterfly *Vanessa cardui* express three rhodopsins homologous to the three *Manduca* visual pigments. The disposition of photoreceptors in the *Vanessa* retina is also similar to that seen in *Manduca*: blue-sensitive cells are concentrated in the ventral half (Briscoe et al., 2003). Briscoe et al. suggested that the retinas of *Vanessa* and *Manduca* may be closer to the ancestral lepidopteran retina than that of *Papilio*, in which six opsins are provided by gene duplication (Briscoe, 1998, 1999, 2000, 2001). In the same vein, we suggest that the similar patterns of regionalization seen in *Manduca* and *Vanessa* may be closer to the ancestral organization of the lepidopteran retina than the more elaborately heterogeneous retinas of butterflies in which opsin gene duplication and chromatic filtering by screening pigments provide additional red- and violet-sensitive receptors (Arikawa and Stavenga, 1997; Arikawa et al., 1999a,b; Qui et al., 2002; Stavenga et al., 2001; Stavenga, 2002a,b).

Rhodopsins of the dorsal rim

Only about one-third of the *dv* cells in the dorsal rim area express P357, and the remaining cells express none of the three opsins that we have characterized from cDNA sequences. There must be one or more opsins expressed in the *Manduca* retina that remain unidentified.

Neuro-behavioral implications

Dusk- and night-active hawkmoths like *Manduca* depend on their well-developed olfactory and visual sensory systems to forage at night-blooming 'hawkmoth flowers' (White et al., 1994; Raguso and Willis, 2002). The visual component of spontaneous foraging behavior in *Manduca* is driven mainly by blue-sensitive receptors (Cutler et al., 1995). The details of the retinal mosaic support our hypothesis (Bennett et al., 1997) that the ventral retina plays a particular role in foraging. The spontaneous feeding behavior of butterflies is also dominated by blue receptors (Scherer and Kolb, 1987a,b), which, as indicated above, are also concentrated in the ventral retina of the butterfly *Vanessa*.

Arikawa and Uchiyama (1996) proposed that *dv* and *pr* cells mediate color vision in the butterfly *Papilio xuthus*. They pointed out that the axons of the *dv* and *pr* cells in Lepidoptera project to the medulla as long visual fibers, whereas *ap* and *ob* cells terminate in the lamina (Ribi, 1987; Bandai et al., 1992; Shimohigashi and Tominaga, 1986, 1991, 1999). Wavelength discrimination in flies may be mediated by receptors giving rise to long visual fibers (Strausfeld and Lee, 1991). Although more recent analysis indicates that other receptors in the *Papilio* retinula must be involved in wavelength discrimination (Kelber, 1999), the original hypothesis of Arikawa and Uchiyama may be relevant to the visual system of *Manduca*, especially if it represents a simpler ancestral organization than that of *Papilio*. The spectral sensitivity of spontaneous foraging in *Manduca* peaks in the blue, has a low shoulder in the green and cuts off sharply at 400 nm (Cutler et al., 1995). The addition of UV wavelengths to mock flowers or illuminated feeding stations hinders foraging (White et al., 1994). These features of the spectral sensitivity of flower visitation may arise from neuronal interactions in the medulla that combine a large positive component from the blue-sensitive *dv* cells, a lesser contribution from the small, green-sensitive *pr* cells and an antagonistic influence from the UV-sensitive *dv* receptors.

Arikawa, Stavenga and associates (Arikawa and Stavenga, 1997; Arikawa et al., 1999b; Qiu et al., 2002; Stavenga, 2002a,b) have argued that the heterogeneous retinal organization of butterfly eyes is associated with color vision; a sensory modality likely to be localized to the ventral retina in some species of these diurnal nectar feeders (Kinoshita et al., 1999). We have shown a similar heterogeneity in the retinal mosaic of *Manduca*. Although *Manduca*'s spontaneous foraging behavior demonstrates only wavelength discrimination, is true color vision also a possibility? Perhaps, because Kelber et al. (2002) have recently found that the hawkmoth *Deilephila elpenor* can employ color vision for foraging under nocturnal light intensities. The fine-grained map of photoreceptor distribution across the *Manduca* retina that we have presented here will benefit further investigation into the remarkable capacities of scotopic vision in hawkmoths.

Appendix: calculation of ratios of P520, P450 and P357 in domains of the yellow retina

The amount of visual pigment in a receptor cell should be proportional to the area of rhabdomeric membrane. Since it is composed of uniform microvilli, the area of membrane in a rhabdomere is proportional to its volume (White and Lord, 1975). Hence, given reasonable assumptions, the rhodopsin ratio in a particular retinal domain can be represented by the ratio of the volumes of the rhabdomeres in the cells that express each rhodopsin.

The volume of rhabdomeres in cells expressing P520 (V_{520}) is the same in all domains of the main retina and is the sum of the rhabdomere volumes from Fig. 3 for the *ap*, *ob* and *pr* cells (V_{ap}, V_{ob} and V_{pr}, respectively). As calculated for a population of 100 retinulae:

$$V_{520} = 100(2V_{ap} + 4V_{ob} + V_{pr}) = 629\,700\ \mu m^3 .$$

The corresponding volumes of rhabdomeres containing P450 and P357 retinulae in a particular retinal domain are represented by the rhabdomere volume of a *dv* cell (V_{dv}) from Fig. 3 multiplied by the relative numbers of *dv* cells (Table 2) expressing P450 or P357 in 100 retinulae of that domain. Thus, for the dorsal domain (Fig. 10B):

$$V_{450} = 33.2 \times V_{dv} = 52\,257\ \mu m^3 ,$$

$$V_{357} = 64.3 \times V_{dv} = 101\,208\ \mu m^3 ,$$

for the dorsal domain just above the equator (Fig. 10E):

$$V_{450} = 38.1 \times V_{dv} = 59\,969\ \mu m^3 ,$$

$$V_{357} = 111.1 \times V_{dv} = 174\,871\ \mu m^3 ,$$

for the ventral domain just below the equator (Fig. 10E):

$$V_{450} = 117.6 \times V_{dv} = 185\ 102\ \mu m^3\ ,$$

$$V_{357} = 59.7 \times V_{dv} = 93\ 968\ \mu m^3\ ,$$

and for the ventral domain (Fig. 10C):

$$V_{450} = 136.9 \times V_{dv} = 215\ 481\ \mu m^3\ ,$$

$$V_{357} = 62.4 \times V_{dv} = 98\ 218\ \mu m^3\ .$$

Rhodopsin ratios for each domain are estimated from the proportions of rhabdomere volumes:

$$\text{P520:P450:P357} = V_{520}/(V_{520} + V_{450} + V_{357}):V_{450}/(V_{520} + V_{450} + V_{357}):V_{357}/(V_{520} + V_{450} + V_{357})\ .$$

Dorsal domain: P520:P450:P357=80:7:13.

Dorsal domain just above the equator: P520:P450:P357= 73:7:20.

Ventral domain just below the equator: P520:P450:P357= 69:20:10.

Ventral domain: P520:P450:P357=67:23:10.

Many thanks are due to William Haber, Robert Stevenson and Adriana Briscoe for varied contributions of expertise. Undergraduates who have contributed include Andrea Hurley, Christine Taylor, Diane Cutler, Samuel Caraballo, Kathryn Johnson, Amanda Birdsey, Lidia Faverman and Ivana Djuretic. This work was supported by NSF grants IBN-9874493 and DBI-9734832.

References

Anton-Erxleben, F. and Langer, H. (1988). Functional morphology of the ommatidia in the compound eye of the moth, *Antheraea polyphemus* (Insecta, Saturniidae). *Cell Tissue Res.* **252**, 385-396.

Arikawa, K. and Stavenga, D. G. (1997). Random array of colour filters in the eyes of butterflies. *J. Exp. Biol.* **200**, 2501-2506.

Arikawa, K. and Uchiyama, H. (1996). Red receptors dominate the proximal tier of the retina in the butterfly *Papilio xuthus*. *J. Comp. Physiol. A* **178**, 55-61.

Arikawa, K., Mizuno, S., Scholten, D. G. W., Kinoshita, M., Seki, T., Kitamoto, J. and Stavenga, D. G. (1999a). An ultraviolet absorbing pigment causes a narrow-band violet receptor and a single-peaked green receptor in the eye of the butterfly *Papilio*. *Vision Res.* **39**, 1-8.

Arikawa, K., Scholten, D. G., Kinoshita, M. and Stavenga, D. G. (1999b). Tuning of photoreceptor spectral sensitivities by red and yellow pigments in the butterfly *Papilio xuthus*. *Zool. Sci.* **16**, 17-24.

Bandai, K., Arikawa, K. and Eguchi, E. (1992). Localization of spectral receptors in the ommatidium of butterfly compound eye determined by polarization sensitivity. *J. Comp. Physiol. A* **171**, 289-297.

Banister, M. J. and White, R. H. (1987). Pigment migration in the compound eye of *Manduca sexta*: effects of light, nitrogen and carbon dioxide. *J. Insect Physiol. A* **33**, 733-743.

Bennett, R. R. and Brown, P. K. (1985). Properties of the visual pigments of the moth *Manduca sexta* and the effects of two detergents, digitonin and CHAPS. *Vision Res.* **25**, 1771-1781.

Bennett, R. R. and White, R. H. (1989). Influence of carotenoid deficiency on visual sensitivity, visual pigment and P-face particles of photoreceptor membrane in the moth *Manduca sexta*. *J. Comp. Physiol. A* **164**, 321-331.

Bennett, R. R., White, R. H. and Meadows, J. (1997). Regional specialization in the eye of the sphingid moth *Manduca sexta*: blue sensitivity of the ventral retina. *Vis. Neurosci.* **14**, 523-526.

Briscoe, A. D. (1998). Molecular diversity of visual pigments in the butterfly *Papilio glaucus*. *Naturwissenshaften* **85**, 33-35.

Briscoe, A. D. (1999). Intron splice sites of *Papilio glaucus PglRh3* corroborate insect opsin phylogeny. *Gene* **230**, 101-109.

Briscoe, A. D. (2000). Six opsins from the butterfly *Papilio glaucus*: molecular phylogenetic evidence for paralogous origins of red-sensitive visual pigments in insects. *J. Mol. Evol.* **51**, 110-121.

Briscoe, A. D. (2001). Functional diversification of lepidopteran opsins following gene duplication. *Mol. Biol. Evol.* **18**, 2270-2279.

Briscoe, A. D. and Chittka, L. (2001). The evolution of color vision in insects. *Annu. Rev. Entomol.* **46**, 471-510.

Briscoe, A. D., Bernard, G. D., Szeto, A. S., Nagy, L. M. and White, R. H. (2003). Not all butterfly eyes are created equal: rhodopsin absorption spectra, molecular identification and localization of UV- blue- and green-sensitive rhodopsin encoding mRNAs in the retina of *Vanessa cardui*. *J. Comp. Neurol.* **458**, 334-349.

Carlson, S. D., Steeves, H. R., Vandeberg, J. S. and Robbins, W. E. (1967). Vitamin A deficiency: effect on retinal structure of the moth *Manduca sexta*. *Science* **158**, 268-270.

Chase, M. R., Bennett, R. R. and White, R. H. (1997). Three opsin-encoding cDNAs from the compound eye of *Manduca sexta*. *J. Exp. Biol.* **200**, 2469-2478.

Cutler, D. E., Bennett, R. R., Stevenson, R. D. and White, R. H. (1995). Feeding behavior in the nocturnal moth *Manduca sexta* is mediated mainly by violet receptors, but where are they located in the retina? *J. Exp. Biol.* **198**, 1909-1917.

Eguchi, E. (1982). Retinular fine structure in compound eyes of diurnal and nocturnal sphingid moths. *Cell Tissue Res.* **223**, 29-42.

Gordon, W. C. (1977). Microvillar orientation in the retina of the nymphalid butterfly. *Z. Naturforsch. C* **32**, 662-664.

Haber, W. A. and Frankie, G. W. (1989). A tropical hawkmoth community: Costa Rican dry forest Sphingidae. *Biotropica* **21**, 155-172.

Janzen, D. H. (1984). Two ways to be a tropical big moth: Santa Rosa saturniids and sphingids. In *Oxford Surveys in Evolutionary Biology*, vol. 1 (ed. R. Dawkins and M. Ridley), pp. 85-140. Oxford: Oxford University Press.

Johnas, W. (1910). Das Facettenauge der Lepidopteren. *Zeitschr. Wiss. Zool.* **97**, 218-261.

Kelber, A. (1999). Ovipositing butterflies use a red receptor to see green. *J. Exp. Biol.* **202**, 2619-2630.

Kelber, A., Thunell, C. and Arikawa, K. (2001). Polarisation-dependent colour vision in *Papilio* butterflies. *J. Exp. Biol.* **204**, 2469-2480.

Kelber, A., Balkenius, A. and Warrant, E. J. (2002). Scotopic colour vision in nocturnal hawkmoths. *Nature* **419**, 922-925.

Kinoshita, M., Shimada, N. and Arikawa, K. (1999). Colour vision of the foraging yellow swallowtail butterfly *Papilio xuthus*. *J. Exp. Biol.* **202**, 95-102.

Kitamoto, J., Ozaki, K. and Arikawa, K. (2000). Ultraviolet receptors and violet receptors express identical mRNA encoding an ultraviolet-absorbing opsin: identification and histological localization of two mRNAs encoding short wavelength-absorbing opsins in the retina of the butterfly *Papilio xuthus*. *J. Exp. Biol.* **203**, 2887-2894.

Kitamoto, J., Sakamoto, K., Ozaki, K., Mishina, Y. and Arikawa, K. (1998). Two visual pigments in a single photoreceptor cell: identification of visual pigment opsins reveals the spectral receptor array in the retina of the butterfly, *Papilio xuthus*. *J. Exp. Biol.* **201**, 1255-1261.

Kolb, G. (1977). The structure of the eye of *Pieris brassicae* L. (Lepidoptera). *Zoomorph.* **87**, 123-146.

Kolb, G. (1985). Ultrastructure and adaptation in the retina of *Aglais urticae* (Lepidoptera). *Zoomorph.* **105**, 90-98.

Kolb, G. (1986). Retinal ultrastructure in the dorsal rim and large dorsal area of the eye of *Aglais urticae* (Lepidoptera). *Zoomorph.* **106**, 244-246.

Labhart, T. and Meyer, E. P. (1999). Detectors for polarized skylight in insects: a survey of ommatidial specializations in the dorsal rim area of the compound eye. *Microsc. Res. Techniques* **47**, 368-379.

Labhart, T., Meyer, E. P. and Schenker, L. (1992). Specialized ommatidia for polarization vision in the compound eye of cockchafers, *Melolontha melolontha* (Coleoptera, Scarabaeidae). *Cell Tissue Res.* **268**, 419-429.

Labhart, T., Petzold, J. and Hebling, H. (2001). Spatial integration in polarization-sensitive interneurones of crickets: a survey of evidence, mechanisms and benefits. *J. Exp. Biol.* **204**, 2423-2430.

Maida, T. M. (1977). Microvillar orientation in the retina of a pierid butterfly. *Z. Naturforsch. C* **32**, 660-661.

Meinecke, C. C. (1981). The fine structure of the compound eye of the African army worm moth, *Spodoptera exempta* (Lepidoptera, Noctuidae). *Cell Tissue Res.* **216**, 333-347.

Qiu, X., Stavenga, D. G. and Arikawa, K. (2002). Ommatidial heterogeneity in the compound eye of the male small white butterfly, *Pieris rapae crucivora*. *Cell Tissue Res.* **307**, 371-379.

Raguso, R. A. and Willis, M. A. (2002). Synergy between visual and olfactory cues in nectar feeding by naïve hawkmoths, *Manduca sexta*. *Anim. Behav.* **64**, 685-695.

Ribi, W. A. (1978). Ultrastructure and migration of screening pigments in the retina of *Pieris rapae* L. (Lepidoptera, Pieridae). *Cell Tissue Res.* **191**, 57-73.

Ribi, W. A. (1987). Identification of spectral receptor types in the retina and lamina of the Australian orchard butterfly, *Papilio aegeus aegeus* D. *Cell Tissue Res.* **247**, 393-407.

Scherer, C. and Kolb, G. (1987a). Behavioral experiments on the visual processing of color stimuli in *Pieris*. (Lepidoptera). *J. Comp. Physiol. A* **160**, 645-656.

Scherer, C. and Kolb, G. (1987b). The influence of color stimuli on visually controlled bin *Aglais urticae* L. and *Pararge aegertia* L. (Lepidoptera). *J. Comp. Physiol. A* **161**, 891-898.

Schlecht, P. (1979). Colour discrimination in dim light: an analysis of the photoreceptor arrangement in the moth *Deilephila*. *J. Comp. Physiol. A* **129**, 257-267.

Schlecht, P., Hamdorf, K. and Langer, H. (1978). The arrangement of colour receptors in a fused rhabdom of an insect. A microspectrophotometric study on the moth *Deilephila*. *J. Comp. Physiol. A* **123**, 239-243.

Shimohigashi, M. and Tominaga, Y. (1986). The compound eye of *Parnara guttata* (Insecta, Lepidoptera, Hesperiidae): fine structure of the ommatidium. *Zoomorph.* **106**, 131-136.

Shimohigashi, M. and Tominaga, Y. (1991). Synaptic organization in the lamina of the superposition eye of a skipper butterfly, *Parnara guttata*. *J. Comp. Neurol.* **408**, 107-124.

Shimohigashi, M. and Tominaga, Y. (1999). Identification of UV, green and red receptors, and their projection to lamina in the cabbage butterfly, *Pieris rapae*. *Cell Tissue Res.* **247**, 49-59.

Stavenga, D. G. (1992). Eye regionalization and spectral tuning of retinal pigments in insects. *Trends Neurosci*. **15**, 213-218.

Stavenga, D. G. (2002a). Reflections on the colourful ommatidia of butterfly eyes. *J. Exp. Biol.* **205**, 1077-1085.

Stavenga, D. G. (2002b). Colour in the eyes of insects. *J. Comp. Physiol. A* **188**, 337-348.

Stavenga, D. G., Kinoshita, M., Yang, E.-C. and Arikawa, K. (2001). Retinal regionalization and heterogeneity of butterfly eyes. *Naturwissenschaften* **88**, 477-481.

Strausfeld, N. J. and Lee, J.-K. (1991). Neuronal basis for parallel visual processing in the fly. *Vis. Neurosci.* **7**, 13-33.

Welsch, B. (1977). Ultrastructur und functionelle Morphologie der Augen des Nachfalters *Deilephila elpenor* (Lepidoptera, Sphingidae). *Cytobiology* **14**, 378-400.

White, R. H. (1961). Analysis of the development of the compound eye in the mosquito, *Aedes aegypti*. *J. Exp. Zool.* **148**, 223-240.

White, R. H. and Bennett, R. R. (1989). Ultrastructure of carotenoid deprivation in photoreceptors of *Manduca sexta*: myeloid bodies and intracellular microvilli. *Cell Tissue Res.* **257**, 519-528.

White, R. H. and Lord, E. (1975). Diminution and enlargement of the mosquito rhabdom in light and darkness. *J. Gen. Physiol.* **65**, 583-598.

White, R. H., Brown, P. K., Hurley, A. K. and Bennett, R. R. (1983). Rhodopsins, retinula cell ultrastructure, and receptor potentials in the developing compound eye of the moth *Manduca sexta*. *J. Comp. Physiol. A* **150**, 153-163.

White, R. H., Stevenson, R. D., Bennett, R. R., Cutler, D. E. and Haber, W. A. (1994). Wavelength discrimination and the role of ultraviolet vision in the feeding behavior of hawkmoths. *Biotropica* **26**, 427-435.

Wolff, T. and Ready, D. F. (1993). Pattern formation in the *Drosophila* retina. In *The Development of* Drosophila melanogaster, vol. 2 (ed. M. Bate and A. M. Arias), pp. 1277-1325. New York: Cold Spring Harbor Laboratory Press.